4f level has been found to be shifted (relative to the bulk value) to higher binding energy for Ta,[26c] but to lower binding energy for W,[26b] IR,[26c] and Au.[26a]

The straightforward bulk-surface computations also reproduce the above crossover behavior. For instance, the renormalized-atom model calculations on Ni[27] have shown "a flow of charge onto the surface site" reducing the d-hole count from its bulk value. Further, the latest ab initio (no pseudopotentials or other empirical forms are used) nine-layer calculations on the Cu(100)[28a,b] and Ni(100)[28c] surfaces reveal the edge bands predominantly of d-electron character, which is consistent with the core shift upward at the surfaces (as found for Au,[26a] Ir,[26c] and W[26b]). At the same time, the similar ab initio 11-layer calculations on Sc(0001) and Ti(0001) surfaces[29] predict the opposite sign for surface core shifts (as found for Ta[26c]), the occupancy of the surface states for Sc being smaller than that for Ti. All the above results agree with our model expectations.

Conclusion

We have to distinguish two aspects of the $(sd)^x$ model, quantitative and qualitative. Quantitatively, the s^1, $(sd)^1$, and $(sd)^x$ models may give rather different numbers. Qualitatively, these models lead to the similar conclusions concerning the surface vs. bulk charge distributions, showing very encouraging agreement with the known theoretical and experimental results. The main disagreement with other authors concerns the charge distributions in some particular model clusters. However, first, we are not interested in these hypothetical clusters themselves (but only as subject to extrapolations), and, second, the effective charge is not a well-defined property and cannot be directly observed and determined even in molecules,[30] not to mention the solids.[31] For this reason, some of the above contridictions may be a mere artifact of the concept used. We think that the best way to proceed is to compare the consequences of all model (computational) conclusions with various experimental (observable!) properties. These include energy and the density of states in the relevant two- and three-dimensional Brillouin zones as well as the differences in work functions[32] and other properties (first of all, catalytic activity) of different surfaces of the same metal, for instance, fcc (111), (110), (001), etc. We will discuss the application of our model to these aspects elsewhere.[10b,33]

Acknowledgments. The authors acknowledge useful discussions with Ralph H. Young.

Appendix

Extended Hückel calculations[34] were performed in the standard manner, using the Wolfsberg–Helmholz formula for off-diagonal matrix elements with a constant value 1.75. Double ζ Slater orbitals were used to represent d orbitals with single Slater functions for the s and p. Standard parameters[35] were employed throughout, and the Mulliken-type analysis was used to determine the charge distribution. The CNDO calculations[36] were performed according to previous work.[37]

(27) Fulde, P.; Luther, A.; Watson, R. E. *Phys. Rev. B* **1973**, *8*, 440.
(28) (a) Gay, J. G.; Smith, J. R.; Arlinghaus, F. J. *Phys. Rev. Lett.* **1979**, *42*, 332. (b) Smith, J. R.; Gay, J. G.; Arlinghaus, F. J. *Phys. Rev. B* **1980**, *21*, 2201. (c) Arlinghaus, F. J.; Gay, J. G.; Smith, J. R. *Phys. Rev. B* **1980**, *21*, 2055.
(29) (a) Feibelman, P. J.; Hamann, D. R. *Solid State Commun.* **1979**, *31*, 413. (b) Feibelman, P. J.; Appelbaum, J. A.; Hamann, D. R. *Phys. Rev. B* **1979**, *20*, 7433.
(30) See, for instance (a) Politzer, P.; Mulliken, R. *J. Chem. Phys.* **1971**, *55*, 5135. (b) Bader, R. F. W. *J. Am. Chem. Soc.* **1971**, *93*, 3095.
(31) Metal solids have the band structure (with the zero energy gap) whose occupancy is determined by the fixed Fermi level, which is the same for the bulk and all surfaces. Therefore, it is usually accepted that surface remains electroneutral, though an effective (electrostatic screening) potential of the surface atoms should be changed with respect to that of the bulk ones, mainly owing to the bulk vs. surface redistribution of the strongly localized d density (d holes).[26-29] Because the d redistribution seems to be rather insensitive to the s, p redistributions even in transition metal alloys,[25b] the former, we hope, can be treated in terms of effective charges.
(32) The differences in work functions for different surfaces cannot be explained by their effective charges only (whatever sign they would have!), but some polarization must be considered (in particular, the formation of the p-(sd) hybrid orbitals), creating a surface dipole moment.[10b]
(33) Baetzold, R. C.; Shustorovich, E., submitted to *Surf. Sci.*
(34) Hoffmann, R. *J. Chem. Phys.* **1963**, *39*, 137.
(35) See, for instance, Baetzold, R. C. *J. Chem. Phys.* **1978**, *68*, 555.
(36) Pople, J. A.; Santry, D. P.; Segal, G. A. *J. Chem. Phys.* **1965**, *43S*, 129.
(37) Baetzold, R. C. *J. Chem. Phys.* **1971**, *55*, 4363.

Intrinsic Barriers in Nucleophilic Displacements

Mark J. Pellerite and John I. Brauman*

Contribution from the Department of Chemistry, Stanford University, Stanford, California 94305. *Received December 28, 1979*

Abstract: Measured rate constants and RRKM theory have been used to estimate central barrier heights in the double-minimum potential surfaces for several gas-phase S_N2 reactions. It is proposed that the barrier heights may be interpreted using the rate–equilibrium relationship originally developed by Marcus, and that the concept of intrinsic barriers embodied in this formalism can be useful when applied to nucleophilic displacements. The results are used to interpret alkoxide and fluoride nucleophilicities and leaving-group abilities.

Nucleophilic displacement reactions have been a fundamental part of organic chemistry for many years. Since the pioneering studies of Hughes and Ingold,[1] much effort has gone into kinetic studies of S_N2 reactions in the hope of developing structure–reactivity correlations. The Swain–Scott relation,[2a] the Edwards equation,[2b] and HSAB theory[2c] have all been used in attempts to correlate reactivity with structural or thermodynamic properties. Success of these correlations is rather limited, as absolute and even relative rates of S_N2 reactions have been found to be highly solvent

(1) Ingold, C. K. "Structure and Mechanism in Organic Chemistry"; Cornell University Press: Ithaca, N.Y., 1969; p 422 ff.
(2) (a) Swain, C. G.; Scott, C. C. *J. Am. Chem. Soc.* **1953**, *75*, 141. (b) Edwards, J. D. *Ibid.* **1956**, *78*, 1819. (c) Pearson, R. G.; Songstad, J. *Ibid.* **1967**, *89*, 1827.

0002-7863/80/1502-5993$01.00/0

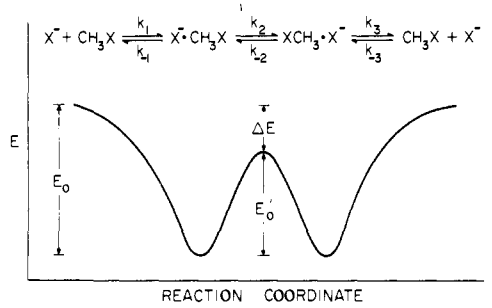

Figure 1. Double-minimum potential surface for a degenerate gas-phase S_N2 reaction.

dependent. This underscores the difficulties involved in elucidating intrinsic (solvent-free) properties of molecules and transition states based on experiments performed in solution.

Solution-phase data have also been used in attempts to describe nucleophilicities and leaving-group abilities in terms of structural and thermodynamic properties. However, here again interference by solvent makes it difficult to distinguish intrinsic properties from solvation effects. For instance, it has long been recognized that alkoxide and fluoride ions almost never participate as leaving groups in S_N2 reactions. Several explanations are generally offered for this behavior. Since the anions are strongly basic, their displacements by most common nucleophiles are believed to be endothermic and hence proceed slowly due to large thermodynamic barriers. Differential solvation effects have also been invoked. We report here the results of some work which indicate that, even in the absence of solvent, alkoxides and fluoride are poor leaving groups. Our treatment shows that there are large intrinsic barriers to alkoxide and fluoride displacements in the gas phase even when effects of solvation and thermodynamics have been eliminated.

Several studies of gas-phase S_N2 reactions have appeared in the literature.[3-8] The available data indicate that rate constants and efficiencies[9] for these reactions can vary over a range of at least three orders of magnitude. This behavior contrasts with gas-phase proton transfers between small ions and molecules, which generally proceed at or near the ion–molecule collision rates.[10] In the initial work from our laboratory,[6,8] we studied by ion cyclotron resonance (ICR) spectrometry[11,12] the reactions of several nucleophiles with a variety of methyl substrates and proposed the double minimum potential surface shown in Figure 1. This is the simplest type of surface which is consistent with available data and still able to account for the wide range of efficiencies observed among the reactions studied.

A complete discussion of the double well potential surface is given in the original work[8,13] and in subsequent papers.[14,15] Consider the thermoneutral displacement reaction shown in Figure 1. As the reactants approach one another, long-range ion–induced dipole and ion–dipole interactions produce a drop in potential energy prior to any chemical barriers produced by orbital overlap. Symmetry considerations require an identical drop on the products side. The intermediates at the potential minima are believed to be loose ion–molecule association complexes. They are relatively long lived and can be observed in three-body association reactions at high pressure, but at the low pressures used in ICR (10^{-6}–10^{-5} torr) they are chemically activated and hence decompose. Within the framework of this model, there is then a potential energy increase up to the central transition state:

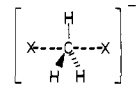

This central barrier is the critical feature of the double-minimum model, and the barrier height is the major factor responsible for the wide variation in efficiencies. A potential barrier lower than the reactants' energy can slow down product formation not because of energetics, which favors products, but because of entropic considerations. Once the activated association complex is formed, dissociation back to reactants (k_{-1}) is more favorable entropically than progress over the central barrier (k_2) since the latter proceeds through a transition state which is much tighter. Thus, the density of states for the k_{-1} channel is larger than that for k_2, since free rotations in the former have been converted to vibrations in the latter.

Nonthermoneutral reactions can also be described with this surface. In these cases, the reactant and product neutrals will in general have different polarizabilities and dipole moments, so the two well depths will also be different.

There is a growing body of work which is consistent with this picture. The existence of barriers to halide exchange in halide–methyl halide adducts has been demonstrated experimentally.[16] Also, this model has proven useful in applications to nucleophilic displacements at carbonyl centers,[14] proton transfer between delocalized anions[13] and hindered pyridine bases,[15] and gas-phase hydrolysis of phosphate esters.[17] Finally, theoretical studies of potential surfaces for several different S_N2 reactions have yielded double-minimum surfaces of this type.[18-21]

Barrier heights in this model are accessible theoretically, given the depth of the initial well. For the three-step mechanism shown in Figure 1, the observed rate constant is[22]

$$k_{obsd} = k_1k_2k_3/[k_{-1}(k_{-2} + k_3) + k_2k_3] \quad (1)$$

For a thermoneutral ion–molecule reaction, k_1 is given by the collision rate constant, $k_{-1} = k_3$, and $k_2 = k_{-2}$ so

$$k_{obsd} = k_1k_2/(k_{-1} + 2k_2) \quad (2)$$

$$\text{efficiency} = k_{obsd}/k_1 = 1/[2 + (k_{-1}/k_2)] \quad (3)$$

For a strongly exothermic reaction, k_{-2} may be neglected[15] relative to k_3:

$$k_{obsd} = k_1k_2/(k_{-1} + k_2) \quad (4)$$

$$\text{efficiency} = k_{obsd}/k_1 = 1/[1 + (k_{-1}/k_2)] \quad (5)$$

Thus, efficiencies can be calculated from the ratio k_{-1}/k_2. This ratio can be calculated[8] as a function of ΔE, the energy difference between the central transition state and the reactants (Figure 1), using RRKM theory.[15,23] Viewed in this light, the problem is reduced to calculating the branching ratio for unimolecular decomposition of the initial adduct into the products (k_2) and reactants (k_{-1}) channels. By repeating the calculation for different values of ΔE, an efficiency vs. ΔE plot is generated. The experimental reaction efficiency may then be fit to this plot to obtain an "experimental" value for ΔE which, given the initial well depth,

(3) Bohme, D. K.; Young, L. B. *J. Am. Chem. Soc.* **1970**, *92*, 7354.
(4) Young, L. B.; Lee-Ruff, E.; Bohme, D. K. *J. Chem. Soc., Chem. Commun.* **1973**, 35.
(5) Bohme, D. K.; Mackay, G. I.; Payzant, J. D. *J. Am. Chem. Soc.* **1974**, *96*, 4027.
(6) Brauman, J. I.; Olmstead, W. N.; Lieder, C. A. *J. Chem. Soc.* **1974**, *96*, 4030.
(7) Tanaka, K.; Mackay, G. I.; Payzant, J. D.; Bohme, D. K. *Can. J. Chem.* **1976**, *54*, 1643.
(8) Olmstead, W. N.; Brauman, J. I. *J. Am. Chem. Soc.* **1977**, *99*, 4219.
(9) Efficiency is defined as the fraction of collisions resulting in reaction: eff = k_{obsd}/k_{coll}.
(10) Lowry, T. H.; Richardson, K. S. "Mechanism and Theory in Organic Chemistry"; Harper and Row: New York, 1976; pp 170–194, and references cited therein.
(11) Baldeschwieler, J. D.; Woodgate, S. S. *Acc. Chem. Res.* **1971**, *4*, 114.
(12) McIver, R. T., Jr. *Rev. Sci. Instrum.* **1978**, *49*, 111.
(13) Farneth, W. E.; Brauman, J. I. *J. Am. Chem. Soc.* **1976**, *98*, 7891.
(14) Asubiojo, O. I.; Brauman, J. I. *J. Am. Chem. Soc.* **1979**, *101*, 3715.
(15) Jasinski, J. M.; Brauman, J. I. *J. Am. Chem. Soc.* **1980**, *102*, 2906.
(16) Riveros, J. M.; Breda, A. C.; Blair, L. K. *J. Am. Chem. Soc.* **1973**, *95*, 4067.
(17) Asubiojo, O. I.; Brauman, J. I.; Levin, R. H. *J. Am. Chem. Soc.* **1977**, *99*, 7707.
(18) Dedieu, A.; Veillard, A. *Chem. Phys. Lett.* **1970**, *5*, 328.
(19) Dedieu, A.; Veillard, A. *J. Am. Chem. Soc.* **1972**, *94*, 6730.
(20) Bader, R. F. W.; Duke, A. J.; Messer, R. R. *J. Am. Chem. Soc.* **1973**, *95*, 7715.
(21) Keil, F.; Ahlrichs, R. *J. Am. Chem. Soc.* **1976**, *98*, 4787.
(22) Eigen, M. *Angew. Chem., Int. Ed. Engl.* **1964**, *3*, 1.
(23) (a) Forst, W. "Theory of Unimolecular Reactions"; Academic Press: New York, 1973. (b) Robinson, P. J.; Holbrook, K. A. "Unimolecular Reactions"; Wiley-Interscience: New York, 1972.

Table I. Rate Constants and Efficiencies

reaction	k^a	$k_{coll}{}^{a,b}$	efficiency^c	k, other work^a	$\Delta H°$, kcal/mol^d
$CH_3O^- + CH_3Cl \rightarrow Cl^- + CH_3OCH_3$	6.03 ± 0.57	19.9	0.30 ± 0.03	4.9,[e] 16,[f] 13[g]	−42
t-$BuO^- + CH_3Cl \rightarrow Cl^- + t$-$BuOCH_3$	1.63 ± 0.16	15.9	0.10 ± 0.01	8.0[f]	−35
$CH_3O^- + CH_3Br \rightarrow Br^- + CH_3OCH_3$	7.27 ± 0.19	18.0	0.40 ± 0.01	7.2,[e] 11[g]	−49
t-$BuO^- + CH_3Br \rightarrow Br^- + t$-$BuOCH_3$	4.06 ± 0.48	13.5	0.30 ± 0.04		−43
$F^- + CH_3Cl \rightarrow Cl^- + CH_3F$	5.84 ± 0.29	23.4	0.25 ± 0.01	8.0,[e] 18,[f] 19[g]	−28

[a] Units of 10^{-10} cm^3/(molecule·s), measured at $T \approx 313$ K. [b] Calculated from ADO theory; see ref 35. [c] k/k_{coll}. [d] Calculated using data from ref 39 and 54. [e] Reference 8. [f] Reference 3. [g] Reference 7.

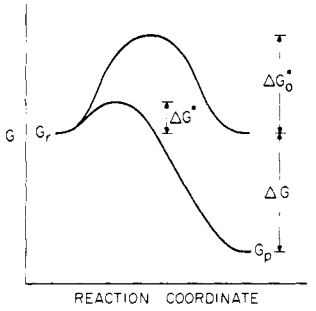

Figure 2. Free-energy barrier as a function of ΔG. Adapted from Murdoch, J. R. *J. Am. Chem. Soc.* **1972**, *94*, 4410.

can be converted into a barrier height. The RRKM calculations are discussed in greater detail in later sections.

We now show that barrier heights calculated by this method can be correlated with exothermicities using a rate–equilibrium relationship, the Marcus equation. One development of this equation begins with the Hammond postulate,[24] which suggests that transition states for strongly exothermic reactions will energetically and geometrically resemble reactants, while those for strongly endothermic reactions will resemble products. Leffler and Grunwald[25] recast this into quantitative form by reasoning that, since a transition state bears some resemblance to reactants and products, changes in its free energy should be linearly related to changes in reactant and product free energies:

$$\delta G^* = \alpha \delta G_p + (1 - \alpha)\delta G_r \qquad (6)$$

where α measures the extent to which the transition state resembles products in terms of its sensitivity to changes in structure or medium.

In an elegant paper, Murdoch[26] has used eq 6 as the starting point for derivation of equations relating the free energy barrier height for an elementary reaction to the exo- or endoergicity and an "intrinsic" barrier, which is the barrier height at $\Delta G = 0$ (Figure 2). An expression for α was also presented. This treatment breaks an activation barrier down into two components—one an intrinsic component, the other arising solely from the overall reaction energetics.[27] The intrinsic barrier for the transfer reaction $AX + B \rightarrow BX + A$ can be regarded as the mean of the barriers for the degenerate exchanges $A + AX \rightarrow AX + A$ and $B + BX \rightarrow BX + B$ under certain conditions.[27] Murdoch lent weight to his equations, which rest on the assumed validity of eq 6, by pointing out that they are equivalent to equations first developed by Marcus[28] for electron-transfer reactions using a quantum-mechanical approach and later extended to atom and group transfers.[27] Thus, the "extended" Hammond postulate[26] and Marcus theory lead to identical results.

There are currently several theories which relate barrier height, exo- or endoergicity, and a parameter α denoting the position along the reaction coordinate at which the transition state occurs.[29] We chose the Marcus theory for our analysis because it is the simplest one which allows interpretation of free-energy barriers in terms of intrinsic and exchange reaction barriers. Although under certain conditions the calculated α's from the various theories can differ significantly, this is of little concern here since we do not interpret the α's physically.

The equations embodied in Marcus theory have been applied to electron-[30] and proton-[27b,31a-d] transfer reactions in solution, S_N2 reactions in solution,[31e] and a few gas-phase atom transfers,[27] with some success. However, no attempt has been made to apply the theory to any gas-phase ion–molecule reactions.[32] We propose that under certain conditions potential surfaces for gas-phase S_N2 reactions may be correlated using Marcus theory.

Reactions we examine here are displacements by F^- on CH_3Cl, and CH_3O^- and t-BuO^- on CH_3Br and CH_3Cl. There are several reasons for choosing these systems. First, although they all proceed at rates substantially below the ion–neutral collision rates, they are efficient enough to be conveniently studied by ICR. Second, the systems are fairly small and of high symmetry and thus are theoretically tractable for RRKM calculations. Finally, all relevant exchange reactions have been dealt with either experimentally[8] or theoretically.[19-21]

Experimental Section

Instrumentation. Rate constants were measured using a pulsed ion cyclotron resonance spectrometer equipped with a trapped-ion cell.[12] Marginal oscillator frequencies were 153.5 or 307 kHz. Total pressures were 10^{-6}–10^{-5} torr, measured with a Varian UHV-24 ionization gauge calibrated in the 10^{-5}–10^{-4}-torr range against an MKS Baratron capacitance manometer.

Determination of Rate Constants. Primary ions were generated by electron impact (0.5–2.0 eV) on a source gas at pressures of $\sim 10^{-7}$ torr. The ions were scanned over time to check for adequate trapping and the absence of unwanted side reactions, and then a known pressure of reactant gas was added. The pseudo-first-order decay of the reactant ion was recorded, and the rate constant was determined from this trace and the reactant gas pressure. This procedure was repeated at different source gas pressures and (except for $CH_3O^- + CH_3Br$) on different days. All reactions were confirmed using double-resonance ion ejection,[12] and the rate constants in Table I are reported as the mean and standard deviation of multiple runs. In some nonexponential decays were observed, especially with the alkoxides. This effect has been observed previously[8,33] and attributed to the presence of vibrationally excited ions. Exponential decay could generally be recovered in these cases by adding $1–2 \times 10^{-6}$ torr of the neutral alcohol, which helped to thermalize the ions through collision and degenerate proton transfer. The rate constants for thermalized ions were larger, accounting for the discrepancy between the rate constant reported here for $CH_3O^- + CH_3Cl$ and that from previous work in our

(24) Hammond, G. S. *J. Am. Chem. Soc.* **1955**, *77*, 334.
(25) (a) Leffler, J. E. *Science* **1953**, *117*, 340. (b) Leffler, J. E.; Grunwald, E. "Rates and Equilibria of Organic Reactions"; Wiley: New York, 1963; p 157.
(26) Murdoch, J. R. *J. Am. Chem. Soc.* **1972**, *94*, 4410.
(27) (a) Marcus, R. A. *J. Phys. Chem.* **1968**, *72*, 891. (b) Cohen, A. D.; Marcus, R. A. *Ibid.* **1968**, *72*, 4249.
(28) Marcus, R. A. *Annu. Rev. Phys. Chem.* **1964**, *15*, 155, and references cited therein.
(29) (a) Agmon, N.; Levine, R. D. *Chem. Phys. Lett.* **1977**, *52*, 197. (b) Agmon, N. *J. Chem. Soc., Faraday Trans. 2* **1978**, *74*, 388, and references cited therein. (c) Miller, A. R. *J. Am. Chem. Soc.* **1978**, *100*, 1984. (d) Agmon, N.; Levine, R. D. *J. Chem. Phys.* **1979**, *71*, 3034.
(30) Weston, R. E.; Schwarz, H. A. "Chemical Kinetics"; Prentice-Hall: Englewood Cliffs, N.J., 1972; Section 7.7.
(31) (a) Marcus, R. A. *J. Am. Chem. Soc.* **1969**, *91*, 7224. (b) Kreevoy, M. M.; Konasewich, D. E. *Adv Chem. Phys.* **1971**, *21*, 243. (c) Albery, W. J.; Campbell-Crawford, A. N.; Curran, J. S. *J. Chem. Soc., Perkin Trans 2* **1972**, 2206. (d) Kreevoy, M. M.; Oh, S.-W. *J. Am. Chem. Soc.* **1973**, *95*, 4805. (e) Albery, W. J.; Kreevoy, M. M. *Adv. Phys. Org. Chem.* **1978**, *16*, 87.
(32) However, for application of the rate–equilibrium relationship developed in ref 29b,c to a unimolecular ion–molecule reaction, see: Schaldach, B.; Grützmacher, H. F. *Int. J. Mass Spectrom. Ion Phys.* **1979**, *31*, 271.
(33) Olmstead, W. N. Ph.D. Thesis, Stanford University, 1976.

Table II. Potential Surface Data for $A^- + CH_3B \rightarrow B^- + CH_3A$

A	B	model, cm^{-1}	ΔE, kcal/mol	barrier height, kcal/mol	ΔG_0^*, kcal/mol	α	ΔG_0^* ($A^- + CH_3A$), kcal/mol[a]
CH_3O	Cl	100	3.1	5.9	21.9	0.26	33.5
		200	5.6	3.4	18.4	0.21	26.6
		300	7.2	1.8	15.8	0.17	21.5
t-BuO	Cl	100	2.4	6.6	21.4	0.28	32.6
		200	3.9	5.1	19.5	0.26	28.8
		300	4.7	4.3	18.3	0.24	26.4
CH_3O	Br	100	3.9	6.1	24.5	0.25	37.8
		200	6.7	3.3	20.5	0.20	29.8
		300	8.6	1.4	17.2	0.14	23.2
t-BuO	Br	100	4.0	6.0	23.3	0.25	35.4
		200	5.8	4.2	20.9	0.22	30.6
		300	6.8	3.2	19.4	0.20	27.6
F	Cl	100	0.9	8.1	19.6	0.32	29.0
		200	2.1	6.9	18.2	0.31	26.2
		300	3.2	5.8	16.9	0.29	23.6

[a] Calculated using $\Delta G_0^*(Cl^- + CH_3Cl) = 10.2$ kcal/mol, $\Delta G_0^*(Br^- + CH_3Br) = 11.2$ kcal/mol, determined (see text) with experimental efficiencies from ref 8. The barrier for $Br^- + CH_3Br$ is only approximate.[8] $\Delta G_0^*(Cl^- + CH_3Cl)$ and $\Delta G_0^*(Br^- + CH_3Br)$ varied little as a function of model; hence the results from the 200-cm^{-1} model were used in all calculations.

laboratory.[8] With no methanol present, we were able to reproduce the previously reported value. On the other hand, our rate constant for $F^- + CH_3Cl$ was consistently found to be ~25% less than the previous value from our laboratory. Although the source of this discrepancy is now known, the different results do not affect our conclusions. No correction for nonreactive ion loss was made for any of these reactions, since they were all sufficiently fast for ion loss to be unimportant.

Materials. NF_3 (Ozark-Mahoning), *t*-BuOO-*t*-Bu (MCB), CH_3Br (Matheson), and CH_3Cl (Matheson) were obtained commercially and used without further purification. CH_3OOCH_3 was prepared according to the procedure of Hanst and Calvert.[34]

Results

The relevant experimental data are shown in Table I. Ion–molecule collision rate constants were calculated using average dipole orientation (ADO) theory.[35] Reliability of the measured rate constants is believed to be about ±30%, due primarily to uncertainty in the Baratron readings below 10^{-4} torr. However, relative rate constants, especially those for different ions reacting with a common substrate, should be much more reliable than this.

Discussion

"Experimental" Barrier Heights. Details of the RRKM calculations appear in the Appendix; however, it is instructive to outline the procedure for one reaction, $CH_3O^- + CH_3Cl$. The branching ratio for decomposition of the reactant collision complex into the k_2 and k_{-1} channels determines the reaction efficiency (eq 5). Since all of the properties of the collision complex cancel out in the calculation, its structure is irrelevant. We need only specify vibrational frequencies, moments of inertia for internal rotors, and external moments for the transition states leading to each of the respective channels. We refer to the k_{-1} transition state as A and that for the k_2 channel as B.

Transition state A is chosen to be the top of the barrier leading to reactants. By microscopic reversibility, this is the point at which the sum of potential and centrifugal energies is a maximum during approach of the ion and neutral.[36a] The separation at which this occurs is approximately[37] the Langevin capture radius,[36b] which at thermal energies is quite large (~6 Å for $CH_3O^- + CH_3Cl$). At this distance the vibrations are those of the separated fragments, accounting for 18 of the 24 internal degrees of freedom. Remaining are the reaction coordinate and five internal rotations. A systematic method which we have developed for treating these rotations is described in the Appendix.

Transition state B is assumed to be

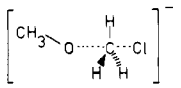

However, if α is interpreted in terms of transition state structure, its value suggests something looser. In assigning frequencies for this structure, CH_3O^- frequences were left unchanged, and those for CH_3Cl were chosen using the previous procedure[8] for CH_3Br. The methyl groups were treated as one-dimensional free rotors on a rigid frame, as outlined by Pitzer.[38] The remaining degrees of freedom are a symmetric O–C–Cl stretch and three bends. Assigning frequencies to these vibrations is difficult, although they must be low[39] (probably under 400 cm^{-1}). Because of this uncertainty three sets of calculations were performed, using values of 100, 200, and 300 cm^{-1} for these frequencies. Input parameters for $CH_3O^- + CH_3Cl$ appear in Table III of the Appendix. Those for the other reactions were chosen analogously.

Figure 3 shows the efficiency vs. ΔE curve for $CH_3O^- + CH_3Cl$ generated with the 200-cm^{-1} model. Fitting the experimental efficiency (Table I) to the curve yields $\Delta E_{exp} = 5.6$ kcal/mol. Now, the initial well depth must be known before the barrier height can be calculated (Figure 1). This well depth corresponds to $\Delta H°$ for the reaction

$$CH_3O^- + CH_3Cl \rightarrow CH_3O^-\cdot CH_3Cl$$

which is not known experimentally. We assume this well depth to be governed primarily by the polarizability and dipole moment of the neutral, and not by the structure of the ion. Dougherty et al.[40] have studied halide–alkyl halide association complexes, and found that those involving CH_3Cl and CH_3Br are bound by 9–10 kcal/mol. We have used well depths of 9 kcal/mol for CH_3Cl complexes and 10 kcal/mol for CH_3Br, expecting errors of no more than 2 kcal/mol or so. Thus, the calculated barrier height for $CH_3O^- + CH_3Cl$ using this model is 9 − 5.6 = 3.4 kcal/mol. The other reactions were treated similarly; results appear in Table II.

Intrinsic Barrier Calculations. The Marcus equations[26-28] are

$$\Delta G^* = [(\Delta G)^2/16\Delta G_0^*] + \Delta G_0^* + \tfrac{1}{2}\Delta G \quad (7)$$

$$\alpha = [\Delta G/8\Delta G_0^*] + 1/2 \quad (8)$$

(34) Hanst, P. L.; Calvert, J. G. *J. Phys. Chem.* **1959**, *63*, 105.
(35) (a) Su, T.; Bowers, M. T. *J. Chem. Phys.* **1973**, *58*, 3027. (b) *Int. J. Mass Spectrom. Ion Phys.* **1973**, *12*, 347.
(36) (a) Waage, E. V.; Rabinovitch, B. S. *Chem. Rev.* **1970**, *70*, 377. (b) Bowers, M. T.; Su, T. In "Interactions between Ions and Molecules", Ausloos, P., Ed.; Plenum Press: New York, 1975; pp 163–183.
(37) The ADO cross section is somewhat larger than the Langevin cross section, but the error introduced by choosing the transition state in this way is not crucial as far as the results of our calculations are concerned.
(38) Pitzer, K. S.; Gwinn, W. D. *J. Chem. Phys.* **1942**, *10*, 428.
(39) Benson, S. W. "Thermochemical Kinetics", 2nd ed.; Wiley-Interscience: New York, 1976; pp 300–302.
(40) (a) Dougherty, R. C.; Dalton, J.; Roberts, J. D. *Org. Mass. Spectrom.* **1974**, *8*, 77. (b) Dougherty, R. C.; Roberts, J. D. *Ibid.* **1974**, *8*, 81. (c) Dougherty, R. C. *Ibid.* **1974**, *8*, 85.

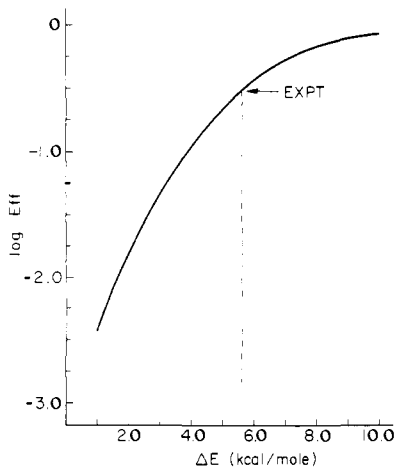

Figure 3. Log efficiency vs. ΔE for $CH_3O^- + CH_3Cl$, 200-cm^{-1} model.

where ΔG^* is the barrier at overall free energy change ΔG, and ΔG_0^* is the intrinsic barrier at $\Delta G = 0$. Since eq 7 and 8 are applicable only to elementary reactions, we apply them to that portion of the potential surface representing passage from the reactant complex $X^-\cdot CH_3Y$ to the product complex $Y^-\cdot CH_3X$. Thus, ΔG is the free-energy difference between the two complexes. When the reactant and product neutrals have similar polarizabilities and dipole moments, this difference will be very close to the overall reaction exothermicity. This is probably the case for reactions of CH_3Cl and CH_3Br with CH_3O^- and F^- but not with t-BuO^- since the polarizability[41] of t-$BuOCH_3$ is about twice that[42] of CH_3Cl or CH_3Br. Since[40c] formation of $Br^-\cdot t$-BuBr is ~3 kcal/mol more exothermic than formation of $Br^-\cdot CH_3Br$, for reactions involving t-BuO^- we have taken the product well to be 3 kcal/mol deeper than the reactant well, and the ΔG's used in eq 7 and 8 are 3 kcal/mol larger than the overall reaction exothermicities.

It should be noted that application of the Marcus theory to these reactions is much more straightforward than application to reactions in solution. Since we are dealing with a single unimolecular step, namely, rearrangement of the reactant complex to the product complex, we need not be concerned with the work terms[28] which must be included in treatments of solution-phase reactions. These terms represent the work required to bring reactants or products to their mean separations in the activated complex, and include Coulombic and desolvation effects.

We now illustrate the use of eq 7 and 8 with the $CH_3O^- + CH_3Cl$, 200-cm^{-1} model. The calculated barrier height is 3.4 kcal/mol, and $\Delta G = \Delta H = -42$ kcal/mol (Tables I and II). Equation 7 can be solved for ΔG_0^*, the intrinsic barrier. Rejecting the quadratic root which leads to a negative α, we are left with $\Delta G_0^* = 18.4$ kcal/mol, $\alpha = 0.21$ for $CH_3O^- + CH_3Cl$. The values for t-$BuO^- + CH_3Cl$ ($\Delta G_0^* = 19.5$ kcal/mol, $\alpha = 0.26$) are similar, as they must be if the model is self-consistent.

The intrinsic barrier is the barrier the reaction would have were it thermoneutral. Following Marcus,[27,28] we can regard the intrinsic barrier for this "cross" reaction as the mean of the barriers for the component "exchange" reactions. Thus, for this case

$$Cl^- + CH_3Cl \rightarrow ClCH_3 + Cl^- \qquad \Delta G_0^*(9) \qquad (9)$$

$$CH_3O^- + CH_3OCH_3 \rightarrow CH_3OCH_3 + OCH_3^- \qquad \Delta G_0^*(10) \qquad (10)$$

$$CH_3O^- + CH_3Cl \rightarrow Cl^- + CH_3OCH_3 \qquad \Delta G_0^*(11) \qquad (11)$$

$$\Delta G_0^*(11) = \tfrac{1}{2}[\Delta G_0^*(9) + \Delta G_0^*(10)] \qquad (12)$$

The Cl^- exchange reaction (9) has also been studied.[8] Using the procedure outlined here, we obtain $\Delta G_0^*(9) = 10.2$ kcal/mol (footnote *a*, Table II). From eq 12, the barrier for methoxide exchange is 26.6 kcal/mol. Intrinsic barriers and α's for the other cross reactions and their associated exchange reactions are given in Table II.

Significance of Intrinsic Barriers. (1) $RO^- + CH_3Cl$, CH_3Br. Several features of these reactions deserve comment. The alkoxide exchange barriers derived from reactions with CH_3Cl and CH_3Br are very similar within a given model, once again demonstrating this treatment's self-consistency. Also, the barriers are quite large, over 20 kcal/mol in all cases. On this basis the alkoxide exchange reactions should be undetectably slow, since such a barrier puts the central transition state at much higher energy than the reactants. Although the t-BuO^- exchange reaction has not been studied, attempts[8] to observe $CD_3O^- + CH_3OCH_3 \rightarrow CD_3OCH_3 + OCH_3^-$ by drift ICR[43] gave no evidence of reaction and an upper limit of 0.0005 on the reaction efficiency. Thus, in accord with our prediction, this alkoxide exchange appears to be too slow to measure. The concept of intrinsic barriers provides insight into why alkoxides are poor leaving groups in solution-phase S_N2 reactions. The methoxide exchange component of the intrinsic barrier for the reaction $X^- + CH_3OCH_3 \rightarrow CH_3X + OCH_3^-$ is so large that regardless of the nature of X^- the reaction is slow unless it is extremely exothermic. As stated earlier, the poor leaving-group ability of alkoxides has in the past been attributed to their high basicity, as displacement of alkoxides by most common nucleophiles is endothermic.[44] However, why do halides displace halides but alkoxides fail to displace alkoxides in thermoneutral reactions? This behavior is generally attributed to greater differential solvation between reactants and transition state in the alkoxide case, since alkoxides are more strongly solvated than halides.[45] Our results require an additional component in the interpretation of alkoxide leaving-group ability and show that solvation is not the only contributing factor. There is a large intrinsic barrier to alkoxide exchange in the gas phase, which in solution is made even larger by differential solvation.

An extremely useful feature of the Marcus treatment is that nucleophilicity and leaving-group ability become equivalent. This can be seen by noting that the *intrinsic* barrier for the general cross reaction $A^- + CH_3B \rightarrow B^- + CH_3A$ is the same in the forward and reverse directions since the thermodynamics have been eliminated. Thus, in the gas phase, alkoxides are also poor nucleophiles; their reactions with CH_3Cl and CH_3Br are fairly efficient only because the reactions are so exothermic. The possible importance of exothermicity in governing rates of S_N2 reactions in solution is still to be explored.

One limitation of the model is that it does not address the question of what makes one exchange barrier higher than another. We have not yet studied enough cases to allow reliable correlations to be made. However, we note that Cl^- and Br^- exchange barriers are lower than those for the alkoxides. It is tempting to attribute this to better charge dispersal and hence transition-state stabilization by the halides, but such conclusions should be regarded as tentative until more reactions involving second-row elements can be studied. Also, this model does not allow us to isolate contributions from transition-state interactions such as steric effects and hard–soft[46] interactions. Steric effects[8] have been observed in gas-phase S_N2 reactions involving only reactants much bulkier than those used here, so for our systems we expect only small steric contributions. Large steric interactions would result in the t-BuO^- exchange barrier being larger than that for CH_3O^- exchange; our results seem to indicate that this is not the case. Hard–soft effects have also been noted for some gas-phase S_N2 reactions,[8] but again

(41) Estimated using data from Denbigh, K. *Trans. Faraday Soc.* **1940**, *36*, 936.
(42) Hirschfelder, J. D.; Curtiss, C. F.; Bird, R. B. "Molecular Theory of Gases and Liquids"; Wiley: New York, 1954; p 947 ff.
(43) (a) Lehman, T. A.; Bursey, M. M. "Ion Cyclotron Resonance Spectrometry"; Wiley-Interscience: New York, 1976; Chapter 1. (b) Smyth, K. C.; Brauman, J. I. *J. Chem. Phys.* **1972**, *56*, 1132.
(44) Streitwieser, A., Jr. "Solvolytic Displacement Reactions"; McGraw-Hill: New York, 1962; p 31.
(45) See, for example, Arnett, E. M.; Johnston, D. E.; Small, L. E. *J. Am. Chem. Soc.* **1975**, *97*, 5598.
(46) Pearson, R. G.; Songstad, J. *J. Am. Chem. Soc.* **1967**, *89*, 1827.

Table III. Data for $CH_3O^- + CH_3Cl$ RRKM Calculations[a]

	transition state A	transition state B
ν_i	2996(6)	2996(6)
	1472(3)	1472(3)
	1455(2)	1455(2)
	1355(1)	1333(1)
	1196(2)	1200(4)
	1020(3)	1029(1)
	732(1)	100(4), 200(4), or 300(4)
I_i, σ_i	19.8, 3(2)	3.0, 3(1)
	34.4, 3(2)	3.1, 3(1)
	0.3, 1(1)	
I_A/I_B	2.05	

[a] Degeneracies are in parentheses. Frequencies (ν_i) are in cm^{-1}, moments of inertia (I_i) are in amu $Å^2$, and σ_i is the symmetry number for the internal rotor.

these were small. For instance,[8] F^- displaces Cl^- from CH_3Cl slightly more efficiently than it displaces Br^- from CH_3Br, even though the former is less exothermic. The same effect has been observed in displacements at carbonyl centers.[14] Within the Marcus framework, reversals such as these may be interpreted as minor breakdown of eq 12. We would expect hard–soft interactions to be reflected in the intrinsic barrier for a cross reaction, and their relative importance indicated by the extent to which eq 12 did not hold. To look for such effects, one would need a system in which barriers to the cross and exchange reactions could be determined directly from experimental efficiencies. Thus far, we know of no such system. Even if one is found, given the uncertainties involved in the calculations it is doubtful that the results would be significant, since available data[8] indicate that such effects are small. In our reactions, hard–soft effects are probably dominated by exothermicity if they are present at all.

(2) $F^- + CH_3Cl$. This reaction was included in our study because the fluoride exchange reaction has been dealt with theoretically, and provides an opportunity to compare barriers estimated by our method with those from ab initio calculations. Dedieu and Veillard[19] have performed an SCF-level potential surface study for $F^- + CH_3F$, and computed a barrier height of 21.1 kcal/mol; their calculated well depth was 13.2 kcal/mol, which is probably too large. Keil and Ahlrichs[21] included electron correlation in their calculation of the energy difference between reactants and transition state; their result was $\Delta E = 8.9$ kcal/mol. Assuming a well depth of 9 kcal/mol leads to a barrier height of 17.9 kcal/mol. Work of Bader et al.[20] produced similar results. Although agreement between these barriers and ours ($\sim$25 kcal/mol) is only marginal, they lie in the same range and indeed are probably equal within the combined uncertainties of both methods. The fluoride exchange barrier is considerably larger than that for chloride, which may be another example of the barrier height–charge dispersal correlation mentioned earlier. Also, as with the alkoxides, our results show that the poor solution phase leaving group ability of fluoride is at least in part an intrinsic property and not due exclusively to solvation and unfavorable thermodynamics as is generally believed.

While this work was in progress, we became aware of very recent work[31e] in which Marcus theory was applied by Albery and Kreevoy to S_N2 reactions at methyl centers in aqueous solution. Experimental activation energies and calculated free energies of reaction were used with the Marcus equation to derive intrinsic barriers for degenerate S_N2 reactions involving several common nucleophiles. Qualitatively, the observed trends agreed with those noted here: the oxygen nucleophiles show large barriers, and the halogen exchange barriers decrease as one moves from fluoride to chloride and bromide. However, actual comparison of the barrier heights is difficult owing to uncertainty in the magnitude of solvent effects. Also, it has recently been shown[47] that intrinsic barriers derived for reactions in solution are sensitive to the rate constants for breakup of the reactant and product encounter complexes. Thus, it is difficult to say whether the intrinsic barriers for the S_N2 reactions in solution are actually representative of the bond-making and bond-breaking process. These points emphasize again that the Marcus equations can only be applied to elementary reaction steps.

(47) Murdoch, J. R. *J. Am. Chem. Soc.* **1980**, *102*, 71.

Conclusion

We propose that potential surfaces for gas-phase S_N2 reactions obey a rate–equilibrium relation, the Marcus equation. Although barrier heights calculated here are probably not quantitatively correct owing to the many uncertainties involved, the concept of intrinsic barriers and exchange reactions embodied in this formalism is one which we believe will prove useful. In particular, our results suggest that the poor leaving-group ability exhibited by alkoxides and fluoride in solution-phase displacements is intrinsic rather than purely a solvation phenomenon.

Our current work is aimed at applying this picture to other S_N2 reactions. Carbanions, delocalized anions, and thioalkoxides are several systems under study. We hope that this will provide a more general picture, and allow other intrinsic barrier–structure trends to be elucidated.

Acknowledgments. We are grateful to the donors of the Petroleum Research Fund, administered by the American Chemical Society, and to the National Science Foundation for support of this research and Fellowship support to M.J.P. We also thank Professor H. C. Andersen for helpful discussions.

Appendix

RRKM equations used in the k_2/k_{-1} calculations have been discussed elsewhere.[8,14,15] Vibrational state sums were calculated using a direct-count procedure for seven frequency groups, and rotations were treated classically.

Input parameters for the $CH_3O^- + CH_3Cl$ calculations appear in Table III. Frequencies and moments of inertia of CH_3Cl are known;[48] those for CH_3O^- were taken[48,49] from CH_3OH and CH_3F. For the other calculations, frequencies and moments of inertia of CH_3Br are known,[48] and those for t-BuO^- were based on t-BuOH, t-BuF, and isobutane.[50,51] The term I_A/I_B in Table III was used in a correction to the internal energy of transition state B as dictated by angular-momentum conservation.[15] I_A was evaluated by treating the fragments as point masses separated by the Langevin capture radius.[36,37]

Internal rotations in transition state A were treated by expressing the partition function Q_{rot}(int) in terms of approximate total rotational and external rotational partition functions:

$$Q_{rot}(\text{int}) = Q_{rot}(\text{total})/Q_{rot}(\text{ext}) \qquad \text{(A-1)}$$

Transition state A consists of two freely rotating fragments separated by a fixed distance. Model calculations showed that in all cases this "molecule" could be treated as a symmetric top since the two largest moments were nearly equal and much larger than the third. Thus, Q_{rot}(ext) is approximately a symmetric top partition function. Coupling between internal and external rotations was accounted for by algebraically averaging the external moments over nine different configurations in which the fragments were oriented with their symmetry axes along one of the three Cartesian axes. The line between the fragment centers of mass was taken as one axis. Q_{rot}(total) was approximated by the product of two partition functions (corresponding to free rotation of the fragments) and a rigid rotor partition function (corresponding to rotation of the whole system approximated by a dumbbell). To include coupling, the external moments for the rigid rotor portion were computed as above by averaging over nine orientations of

(48) Herzberg, G. "Infrared and Raman Spectra of Polyatomic Molecules"; Van Nostrand-Reinhold: Princeton, N.J., 1945; p 315.
(49) Reference 48, p 334 ff.
(50) Mann, D. E.; Acquista, N.; Lide, D. R.; Jr. *J. Mol. Spectrosc.* **1958**, *2*, 575.
(51) Snyder, R. G.; Schachtschneider, J. H. *Spectrochim. Acta* **1965**, *21*, 169.

the fragment molecules. The complete expression is

$$Q_{rot}(\text{int}) = \frac{Q_{st}(I_x(1),I_y(1),I_z(1))Q_{st}(I_x(2),I_y(2),I_z(2))Q_{rr}(I_{x,y}(\text{av,ext}))}{Q_{st}(I_{x,y,z}(\text{av,ext}))} \quad \text{(A-2)}$$

where Q_{st} and Q_{rr} are symmetric top and rigid rotor parition functions. $I_x(1)$, etc., refer to moments of inertia of the fragments, and $I_{x,y}(\text{av,ext})$ and $I_{x,y,z}(\text{av,ext})$ to the external moments averaged over nine fragment molecule orientations. Although eq A-1 is an approximation, it reduces to the correct expression[52,53] when applied to the case of two symmetric coaxial rotors (such as ethane, assuming free rotation).

(52) Reference 39, p 43.
(53) Pitzer, K. S. "Quantum Chemistry"; Prentice-Hall: Englewood Cliffs, N.J., 1953; p 239.
(54) Bartmess, J. E.; McIver, R. T., Jr. In "Gas-Phase Ion Chemistry", Bowers, M. T., Ed.; Academic Press: New York, 1979; Vol. 2, Chapter 11.

Conformations of Six N-Methylated Diketopiperazines in Solution

W. Radding,* B. Donzel, N. Ueyama, and M. Goodman*

Contribution from the Department of Chemistry, B-014, University of California, San Diego, La Jolla, California 92093. *Received May 29, 1979*

Abstract: The conformations of six N-methylated diketopiperazines in solution are determined by a combination of NMR and CD techniques and compared to the results of X-ray crystallography. Of the six compounds, three apparently have conformations in solution substantially different from their conformations in the crystalline state. Strongly protonating solvents apparently do not change the diketopiperazine ring angle of fold. However, solvent effects may dramatically alter the side-chain rotamer populations of the aromatic substituted diketopiperazines.

Introduction

Diketopiperazines, both in the solid state and in solution, have been traditional models for studies of peptides,[1] polypeptides, and proteins.[2] One diketopiperazine is more than a model: cyclo-L-histidyl-L-prolyl (c-L-His-L-Pro) is a degradation product of thyrotropin hormone releasing hormone (THRH) and is itself biologically active.[3] Others are naturally occurring antibiotics.[4,5]

In a previous paper the X-ray structures of six N-methylated diketopiperazines, cyclobis(L-*N*-methylalanyl) [c-(L-NMeAla)$_2$], cyclo-L-methylalanyl-D-*N*-methylalanyl (c-L-NMeAla-D-NMeAla), cyclobis(L-*N*-methylvalyl) [c-(L-NMeVal)$_2$], cyclo-L-*N*-methylvalyl-D-*N*-methylvalyl (c-L-NMeVal-D-NMeVal), cyclobis(L-*N*-methylphenylalanyl) [c-(L-NMePhe)$_2$], and cyclo-L-*N*-methylphenylalanyl-D-*N*-methylphenylalanyl (c-L-NMePhe-D-NMePhe) plus cyclobis(L-valyl) [c-(L-Val$_2$], were reported.[6] The optically active alkyl-substituted compounds exhibit pseudoaxial side chains and a negative diketopiperazine ring fold, $\beta < 0°$ (Figure 1),[7] while the DL isomers assume chair conformations. The steric interaction between the side chains of the optically active isomers is less than that between the individual side chains and the carbonyl or the *N*-methyl groups on the ring. In c-(L-NMeAla)$_2$ and c-L-NMeVal-L-NMeVal, where the CD spectrum can unambiguously determine the sign of the ring fold angle β, it is of particular interest to test the conformations of the diketopiperazines in solution in comparison to the X-ray results, since in one earlier case,[7] cyclobis(L-alanyl) [c-(L-Ala)$_2$], β for the solid is positive in the crystal, while it is negative in solution. In this paper we report circular dichroism (CD) and nuclear magnetic resonance (NMR) spectra obtained from the N-methylated alkyldiketopiperazines to identify the dominant conformations in solution. From these results, we hope to elucidate the important forces determining these conformations.

It is much more difficult to decipher the optical spectroscopy of aryl-substituted diketopiperazines. The study of aryldiketopiperazines in solution by NMR has demonstrated the tendency for the side chains to "hover" over the diketopiperazine ring,[8,9] even in the face of apparent steric repulsion. In two cases, cyclo-L-phenylalanyl-L-tyrosyl (c-L-Phe-L-Tyr) and cyclobis(L-tyrosyl) [c-(L-Tyr)$_2$], it has been proposed that both aromatic chromophores share the space over a diketopiperazine simultaneously for a major fraction of the time.[10] With the problems of spectroscopic interpretation and side-chain interaction in mind and with the information about steric forces available from the alkyl-substituted compounds, we report an analysis of cyclobis(L-*N*-methylphenylalanyl) [c-(L-NMePhe)$_2$] by CD and NMR.

Materials And Methods

Materials. The diketopiperazines c-(L-Ala)$_2$, c-L-Ala-D-Ala, c-(L-Val)$_2$, c-L-Val-D-Val, c-(L-Phe)$_2$, and c-L-Phe-D-Phe were prepared ac-

*Address correspondence to W.R. at the Department of Neurological Surgery, College of Physicians and Surgeons, Columbia University, New York, N.Y. 10032, and to M.G. at the Department of Chemistry, B-104, University of California, San Diego, La Jolla, Calif. 92093.

(1) (a) Pauling, L.; Cory, R. B.; Branson, H. R. *Proc. Natl. Acad. Sci. U.S.A.* **1951**, *37*, 207. (b) Pauling, L.; Cory R. B. *Ibid.* **1951**, *37*, 205. (c) Pauling, L.; Cory, R. B. *Ibid.* **1951**, *37*, 241. (d) Pauling, L.; and Cory, R. B. *Ibid.* **1951**, *37*, 251.
(2) Hooker, T. M.; Goux, W. J. *Jerusalem Symp. Quantum Chem. Biochem.* **1977**, *10*, 123–36. Goux, W. J.; Hooker, T. M. *ABS. Pap. DCS* **1976**, *172*, 62.
(3) Prasadd, C.; Matsui, T.; Peterkol, A. *Nature (London)* **1977**, *268*, 32.
(4) Steyn, P. S. *Tetrahedron* **1973**, *29*, 107.
(5) Johne, S.; Groger, D. *Pharmazie* **1977**, *32*, 1.
(6) Benedetti, E.; Marsh, R. E.; Goodman, M. *J. Am. Chem. Soc.* **1976**, *98*, 6676.
(7) Hooker, T. M., Jr.; Bayley, P. M.; Radding, W.; Schellman, J. A. *Biopolymers* **1971**, *10*, 1973.
(8) Kopple, K. D.; Marr, D. H. *J. Am. Chem. Soc.* **1967**, *89*, 6193.
(9) Kopple, K. D.; Ohnishi, M. *J. Am. Chem. Soc.* **1969**, *91*, 962.
(10) Strickland, E. H.; Wilchek, M.; Horwitz, J.; Billups, C. *J. Biol. Chem.* **1970**, *245*, 4168.

0002-7863/80/1502-5999$01.00/0